Geophysical Research Letters

RESEARCH LETTER
10.1029/2018GL081648

N_2O Emissions From the Northern Benguela Upwelling System

D. L. Arévalo-Martínez[1], T. Steinhoff[1], P. Brandt[2,3], A. Körtzinger[1,3], T. Lamont[4,5], G. Rehder[6], and H. W. Bange[1]

[1]Chemical Oceanography Department, Helmholtz Centre for Ocean Research Kiel, Düsternbrooker Weg 20, Kiel, Germany, [2]Physical Oceanography Department, Helmholtz Centre for Ocean Research Kiel, Düsternbrooker Weg 20, Kiel, Germany, [3]Faculty of Mathematics and Natural Sciences, Kiel University, Kiel, Germany, [4]Department of Environmental Affairs, Oceans and Coasts Research Branch, Cape Town, South Africa, [5]Marine Research Institute and Department of Oceanography, University of Cape Town, Rondebosch, South Africa, [6]Leibniz Institute for Baltic Sea Research Warnemünde, Seestraße 15, Rostock, Germany

Key Points:
- Strong cross-shelf variability of N_2O results from upwelling and advection at discrete centers along the coast
- N_2O fluxes from the northern Benguela region suggest its role as an overall source to the atmosphere
- The contribution of the northern Benguela region to global ocean N_2O emissions might need to be revised upward

Supporting Information:
- Supporting Information S1

Correspondence to:
D. L. Arévalo-Martínez,
darevalo@geomar.de

Citation:
Arévalo-Martínez, D. L., Steinhoff, T., Brandt, P., Körtzinger, A., Lamont, T., Rehder, G., & Bange, H. W. (2019). N_2O emissions from the northern Benguela upwelling system. *Geophysical Research Letters*, *46*, 3317–3326. https://doi.org/10.1029/2018GL081648

Received 11 DEC 2018
Accepted 19 FEB 2019
Accepted article online 22 FEB 2019
Published online 18 MAR 2019

Abstract The Benguela Upwelling System (BUS) is the most productive of all eastern boundary upwelling ecosystems and it hosts a well-developed oxygen minimum zone. As such, the BUS is a potential hotspot for production of N_2O, a potent greenhouse gas derived from microbially driven decay of sinking organic matter. Yet, the extent at which near-surface waters emit N_2O to the atmosphere in the BUS is highly uncertain. Here we present the first high-resolution surface measurements of N_2O across the northern part of the BUS (nBUS). We found strong gradients with a threefold increase in N_2O concentrations near the coast as compared with open ocean waters. Our observations show enhanced sea-to-air fluxes of N_2O (up to 1.67 nmol m^{-2} s^{-1}) in association with local upwelling cells. Based on our data we suggest that the nBUS can account for 13% of the total coastal upwelling source of N_2O to the atmosphere.

Plain Language Summary Nitrous oxide (N_2O), commonly known as "laughing gas," is a potent greenhouse gas that contributes both to Earth's warming and to the depletion of ozone in the stratosphere. Typically, N_2O is produced in the water column as a result of microbial decay of organic matter (under low oxygen conditions) and then it is transferred to the atmosphere at the air-sea interface. Hence, high productive regions associated with low oxygen waters could create "hotspots" for N_2O production. Yet, emission estimates might have underestimated the potential of coastal regions due to data sparcity. We focus on the northern Benguela region, which is the most productive of four major coastal upwelling ecosystems. Here we aim to answer: what is the large-scale distribution and variability of air-sea fluxes of N_2O? What is the impact of small-scale oceanographic features in N_2O variability? and Do regional emissions of N_2O need to be revisited? Based on the analysis of continuous highly resolved measurements, we suggest that the share of this region to the total N_2O emitted by the global ocean is higher than previously thought. Considering that this region represents only 0.06% of the ocean surface, we argue that the marine budget of this gas might need revision.

1. Introduction

Nitrous oxide (N_2O) is a strong greenhouse gas and plays a pivotal role in stratospheric ozone depletion (Myhre et al., 2013; Ravishankara et al., 2009). Among its natural sources, the global open ocean and coastal areas stand out with one third of the total emissions to the atmosphere (Myhre et al., 2013). Yet, most estimates of marine emissions of N_2O report high uncertainties caused by the sparcity of data in areas which emit considerable amounts of this gas during, for instance, upwelling events (Bange et al., 1996; Nevison et al., 2004). From this it follows that a better understanding of the distribution and magnitude of marine emissions of N_2O is required, in particular, when considering the increasing impacts of anthropogenically driven perturbations of the nitrogen cycle in coastal areas worldwide (Gruber & Galloway, 2008; Seitzinger et al., 2000; Suntharalingam et al., 2012; Voss et al., 2013).

Eastern Boundary Upwelling Systems (EBUS) include some of the most productive regions of the ocean, accounting for about 11% of the global new production (Chavez & Toggweiler, 1995). The high productivity

in EBUS results from wind-driven coastal upwelling and mixing by internal waves which transport(mix) cold, nutrient-rich subsurface waters into the euphotic layer, favoring the occurrence of remarkably high levels of planktonic biomass (Carr, 2002; Schafstall et al., 2010). Sinking of this biomass promotes high rates of microbial respiration at depth, which together with slow oxygen (O_2) supply leads to the formation of perennial oxygen minimum zones (OMZ; Capone & Hutchins, 2013). Among EBUS, the Benguela Upwelling System (BUS; 14–34°S) has the highest primary production rates (40% of EBUS contribution to the global ocean net production (Behrenfeld & Falkowski, 1997; Carr, 2002; Monteiro, 2010). Low-O_2 waters above the shelf can be found between 15 and 30°S, but the strongest depletion occurs north of 27°S (Hutchings et al., 2009; Mohrholz et al., 2008; Monteiro & van der Plas, 2006). Since N_2O production is elevated under low O_2 conditions (Elkins et al., 1978; Goreau et al., 1980), OMZ waters in the BUS could create "hotspots" for subsurface N_2O production (Frame et al., 2014; Gutknecht, Dadou, Marchesiello, et al., 2013). Although the BUS is an intense site of N-loss via anammox and denitrification (Kuypers et al., 2005; Nagel et al., 2013), the few available studies on N_2O in this region (Frame et al., 2014; Gutknecht, Dadou, Marchesiello, et al., 2013; Nevison et al., 2004) have shown that this area is a net source to the atmosphere. Nevertheless, previous N_2O emission estimates for the BUS were based either on continuous data gathered far from the influence of coastal upwelling, or on discrete sampling methods which usually overlook small-scale temporal and spatial variability.

Here we present the first continuous, high-resolution measurements of dissolved N_2O across the northern BUS (nBUS) during austral winter. We use the unprecedented data coverage to assess the spatial variability of N_2O concentrations and sea-air fluxes in this region and to investigate how it relates to the occurrence of upwelling filaments. We also provide an updated estimate of N_2O emissions for the region and discuss its significance for the global ocean budget of this gas.

2. Data and Methods

2.1. Study Area

The field work took place during three expeditions on board the RV Meteor (July–September 2013; cruises M98, M99, M100/1), as part of the South African TRace gas Experiment (SATRE). Continuous measurements were carried out during several along- and cross-shelf sections off Angola and Namibia (Figure 1). Since our survey exceeded the northern boundary of the BUS (~16°S; Lutjeharms & Meeuvis, 1987), and for comparison, we divided our study area in three domains: Angola Tropical Zone (ATZ; 10–14°S), Angola-Benguela Front (ABF; 14–16°S), and nBUS (16–28.5°S). The ATZ is a transition band between the equatorial Atlantic and the BUS and it is characterized by seasonal cooling and shoaling of the thermocline (maximum in austral winter) in association with coastally trapped waves (Hutchings et al., 2009; Tchipalanga et al., 2018). The ABF is a thermal front that separates warm, oligotrophic tropical waters of the Angola Current (AC) from cold waters upwelled further south (Mohrholz et al., 2001, 2008). Although upwelling-favorable winds in the BUS occur between 14 and 35°S, the coastal topography and shelf width result in independent cells with enhanced upwelling (Hutchings et al., 2009; Lutjeharms & Meeuvis, 1987). In this study we focus on the nBUS, whose major cells are: Cunene (17°S), Cape frio (18.5°S), northern Namibia (19°S), Walvis Bay (23°S), and Lüderitz (27°S) (Kämpf & Chapman, 2016; Lutjeharms & Meeuvis, 1987). In order to quantitatively express the extent of upwelling events in the nBUS, we used the total cumulative upwelling indices (TCU) from Lamont et al. (2017). TCU are defined as the sum of all offshore Ekman transport values computed for a given latitude, with positive values indicating shoreward transport of subsurface waters (see details on the supporting information; Kanamitsu et al., 2002; Lamont et al., 2017; Trenberth et al., 1990). As can be seen in Figure 1, TCU for the nBUS suggested enhanced upwelling in the vincinity of the major upwelling cells.

2.2. Continuous Measurements of N_2O

Along-track measurements of N_2O (resolution ~0.2 km) were conducted with an autonomous setup which combined the methods by Pierrot et al. (2009) and Arévalo-Martínez et al. (2013). In brief, a GO CO_2 system (General Oceanics Inc., USA) was coupled to an RMT-200 N_2O/CO analyzer (Los Gatos Research Inc., USA), such that the VALCO valve (Vici®) of the former automatically switched between seawater, atmosphere, and reference gases measurement circuits. The gas circulation through the systems was mantained by the RMT-200's internal pump (flow = 250 ml/min). This pump was located downstream of the measurement cells and ensured that the analyzed gas was directed either back to the equilibrator (seawater measurements), to the dry box of the GO system (atmospheric measurements), or to a vent (reference gas

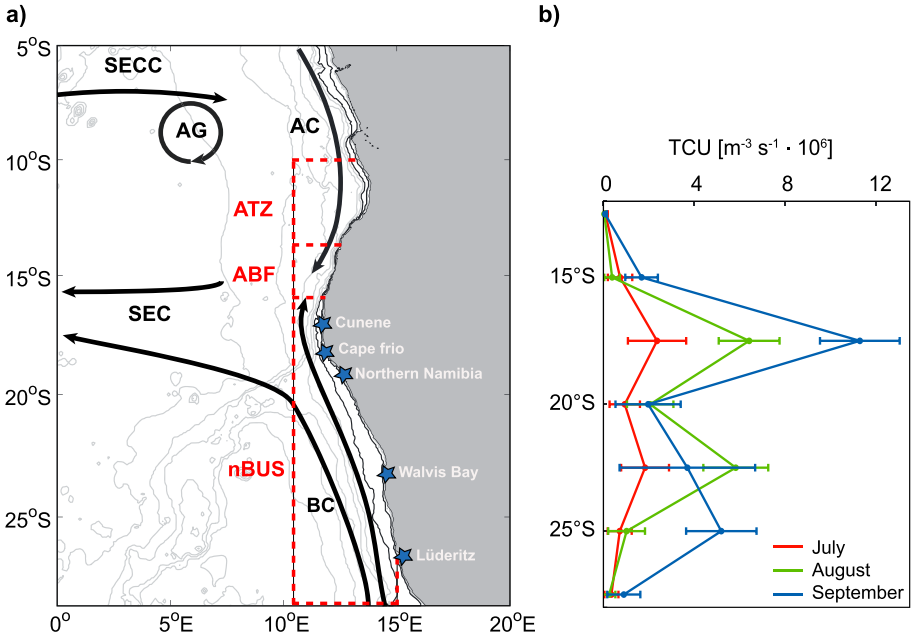

Figure 1. Northern Benguela upwelling system. (a) Red dashed lines enclose the spatial domains considered in this study (ATZ, ABF, nBUS), whereas the main surface circulation features are depicted by black arrows (AC, AG, BC, SEC, SECC). Currents are based on Kopte et al. (2017). (b) TCU for the nBUS at the time of sampling. Values shown are monthly means (±SD) of TCU computed per 100-m coastline at each location. Main upwelling cells are indicated in (a). ATZ = Angola Tropical Zone; ABF = Angola-Benguela Front; nBUS = northern Benguela upwelling system; AC = Angola Current; AG = Angola Gyre; BC = Benguela Current; SEC = South Equatorial Current; SECC = South Equatorial Countercurrent; TCU = Total cumulative upwelling indices.

measurements). Water from ~6 m depth was brought into the system continuously (flow = 2–3 L/min) with a submersible pump mounted at the vessel's hydrographic slot. To correct for warming between intake and equilibrator, the water temperature was monitored with a Sea-Bird SBE38 thermometer (accuracy ±0.001 °C) and a Fluke® 1523 digital thermometer (accuracy ±0.01 °C), respectively. Along-track salinity data were taken from the ship's thermosalinograph (SeaCAT SB21E). Atmospheric N_2O measurements were carried out for 15 min every 6 hr by drawing air from an intake at 35 m height. Two reference gases (362.3 and 746.0 ppb N_2O) calibrated against the World Meteorological Organization standard scale were used for instrument calibration and assessment of instrumental drift (maximal deviation from reference ≤1.5%).

2.3. Data Processing

Data reduction and calibration as well as the calculation of N_2O concentrations followed those from Arévalo-Martínez et al. (2013) and references therein. Atmospheric N_2O data were linearly interpolated over the time of the cruises and then used for the computation of the equilibrium concentrations, saturations, and sea-air fluxes of N_2O. Our mean atmospheric N_2O value (325.7 ± 1.82 ppb) was in good agreement with both flask data from the NOAA's Cooperative Globar Air Sampling Network (325.9 ± 0.38 ppb; 23.58°S, 15.03°E; Dlugokencky et al., 2014) and continuous measurements at the Namib Dessert Atmospheric Observatory (~326 ppb; Morgan et al., 2015). N_2O saturations (N_2O_{sat}) were obtained from the concentration (C) ratio between seawater (sw) and atmospheric equilibrium (atm) values ($N_2O_{sat} = C_{sw}/C_{atm}\cdot 100$). Sea-air flux densities of N_2O (F_{N_2O}) were computed as described in Arévalo-Martínez et al. (2017) with instantaneous wind speeds taken from the ship's weather system (standardized to 10 m height; Garrat, 1977).

3. Results and Discussion

3.1. N_2O Distribution and Regional Variability

Dissolved N_2O fluctuated between 7.8 and 30.9 nmol L^{-1} with enhanced concentrations in the shelf and progressively decreasing values in offshore direction (Figure 2). As in other EBUS (see, e.g., Nevison et al., 2004), marked cross-shelf gradients associated with coastal upwellling were the dominant feature of the surface distribution of N_2O. This is supported by the good agreement between N_2O and sea surface temperature

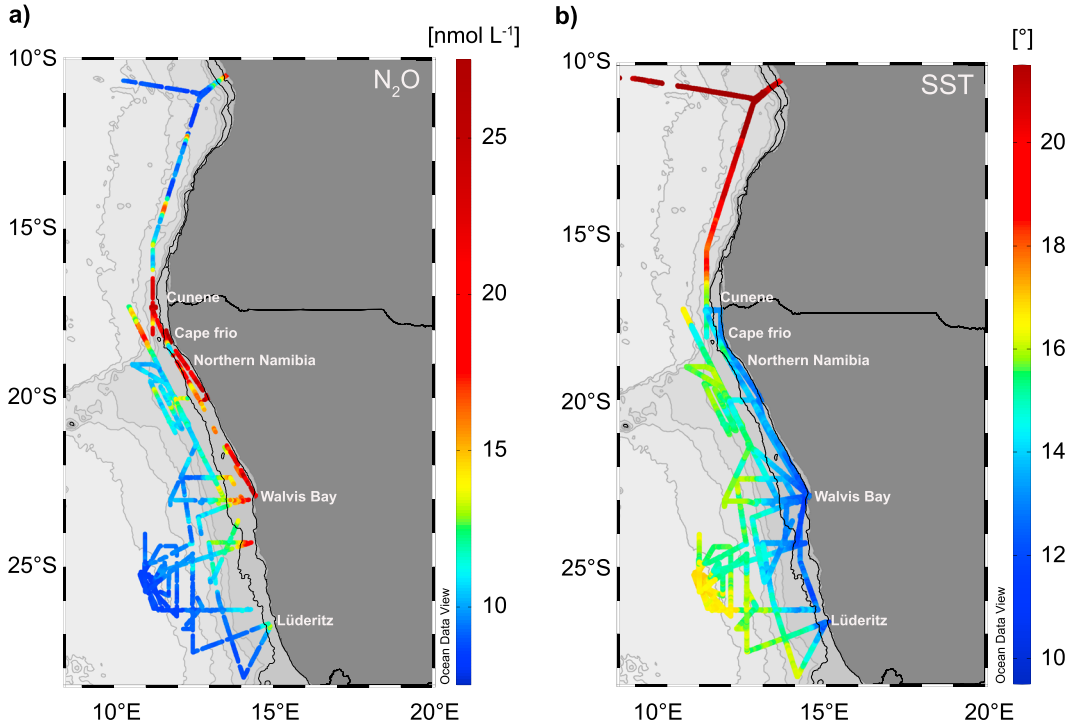

Figure 2. Surface distribution of N_2O in this study. Along-track N_2O concentrations (a) and SST (b) are shown. The location of main upwelling cells is shown and the 50 and 200 m bathymetric contours are indicated by black lines. SST = sea surface temperature.

(SST) throughout the cruises (Figures 2 and S1). Detailed inspection of cross-shelf sections at the ATZ and the nBUS revealed a highly heterogeneous distribution with small-scale (<10 km) variability in the zonal distribution of N_2O as well as marked differences in the shape and magnitude of the gradients. However, overall the highest N_2O concentrations were found within 50 km from the coast (Figure S2).

3.1.1. ATZ

N_2O concentrations in the ATZ were the lowest across the study area (minimum 7.8 nmol L^{-1}), in good agreement with the results of Frame et al. (2014). It is noteworthy, however, that our measurements in the ATZ were conducted mostly out of the shelf. An exception was the section at 11°S in which a sharp N_2O gradient with inshore concentrations up to 19.5 nmol L^{-1} could be observed (Figure S2). Although the 11°S section laid between the Cunene cell and a weaker cell off Luanda (7°S; Lutjeharms & Meeuvis, 1987), the lower N_2O concentrations north and south of the section suggests that the zonal gradient of N_2O resulted from local upwelling, likely driven by the passage of coastally trapped waves which lead to SST cooling in July/August (Kopte et al., 2017). These observations are further supported by outcropping isopycnals from 40 to 50 m depth and O_2 profiles, which show an inshore shoaling of low-O_2 waters (Figure S3; for information on the methods see also Hansen, 1999). These waters correspond to the AC, which transports nutrient-rich O_2-poor South Atlantic Central Waters from the equatorial region and the Angola Gyre southward (Kopte et al., 2017; Mohrholz et al., 2001; Shannon et al., 1987). One further patch of cold waters with increased N_2O concentrations was also observed in the ATZ (12–12.5°S). Although narrow, this patch with low SST could also indicate the presence of an upwelling filament, which is a recurrent feature in this area (Shannon et al., 1987).

3.1.2. ABF

Marked meridional differences of SST and salinity were observed across the ABF (Figure S1). SST ranged between 21.2 °C at about 14°S and 17.7 °C near 16°S, reflecting the transitional character of the frontal zone (Mohrholz et al., 2001). Surface N_2O concentrations were comparable to those of the ATZ (range 7.8–16 nmol L^{-1}) and, except for a narrow band at ~14.5°S, generally lower than those south of the frontal zone. Meandering waters due to mesoscale features such as eddies and filaments are a well-documented phenomenon in the BUS, accounting for most of the observed temporal-spatial variability (Chavez & Messié, 2009). Hence, it is likely that the slightly higher N_2O in the northern boundary of the

ABF resulted from frontal dynamics associated with along-frontal winds rather than from upwelling. Nevertheless, as in the ATZ, most of our measurements in the ABF were carried out at larger distances from the coast as compared with those in the nBUS.

3.1.3. nBUS

The highest N_2O concentrations in this study were observed in the nBUS, in particular on the shelf where dissolved N_2O exceeded atmospheric equilibrium (C_{atm}) values by one order of magnitude (C_{atm} = 7.0–10.4 nmol L^{-1}; Figure 2). The cold water parcels (13–16 °C) which extended westward until about 10.5°E at ~17–18°S (Cunene and Cape frio cells) beared the maximal N_2O concentrations for the nBUS. In coherence with this observation, our TCU for those cells were the highest, reflecting the seasonal upwelling peak (Jury, 2017).

We found reduced N_2O concentrations (minimum 13.7 nmol L^{-1}) and a less steep gradient (Figure S2) in the vincinity of the Lüderitz cell (27°S). Although upwelling off Lüderitz is the strongest in terms of frequency, offshore extension and transport (Lutjeharms & Meeuvis, 1987), its primary productivity is considerably lower than in other cells because strong turbulence prevents the formation of appreciable phytoplanktonic blooms (Hutchings et al., 2009). This suggests that the supply of organic matter (OM) to depth around 27°S is potentially lower than in other cells. Denitrification in sediments, water column nitrification, and nitrifier-denitrification are the main known production pathways for N_2O in the nBUS (Frame et al., 2014; Gutknecht, Dadou, Marchesiello, et al., 2013). Given that these processes rely on the export of OM from the surface, it could be expected that N_2O concentrations at depth were lower in the southern part of the nBUS due to reduced O_2 demand for OM-remineralization (Elkins et al., 1978). Moreover, while the supply of O_2-rich waters from the Eastern South Atlantic Central Water to the shelf increases south of 27°S, the impact of the O_2-poor AC weakens at about the same latitude (Mohrholz et al., 2008). Hence, a combination of increased O_2 supply and reduced consumption might explain the comparatively lower N_2O concentrations in surface waters off Lüderitz.

3.2. N_2O Efflux to the Atmosphere

Most waters (>99% of the observations) were supersaturated with respect to atmospheric equilibrium (N_2O_{sat} = 98–317%), and slight undersaturation was observed only west of 11.5°E. In order to illustrate the zonal variability of N_2O ougassing, we binned our observations in shelf (≤200 m depth), slope (200–1,000 m depth) and open ocean (>1,000 m depth) areas and allocated saturation values to categories of increasing magnitude (Figure 3). Our results show that the overwhelming majority (88%) of shelf waters had saturation values which approach to and surpass doubling C_{atm}, whereas the fraction of waters with these characteristics decreased sharply to 15% and 6% in slope and open ocean areas. Furthermore, moderate enhancement in N_2O_{sat} (120–150%) was more frequent in waters above the slope, suggesting N_2O outgassing as waters warm while transported offshore following upwelling events. Although most of our observations were conducted above slope and open ocean waters (Figure S4), our data clearly show the disproportionately high contribution of upwelling above the shelf, in contrast with recent studies (e.g., Buitenhuis et al., 2018) which suggest coastal systems to have lower-than-expected contributions to N_2O fluxes with respect to their size.

Since the major aim of this work is to discuss the N_2O emissions from the nBUS, in the following we focus on the area between 16 and 28.5°S. F_{N_2O} ranged between −0.03 and 1.67 nmol m^{-2} s^{-1}, with the highest values in areas with upwelling-favorable winds as indicated by the TCU (Figures 1 and 3), and slightly negative values south of 25°S. Although our data lie well within the range of previous estimates, our F_{N_2O} in near-coastal areas were substantially higher. For instance, Gutknecht, Dadou, Marchesiello, et al. (2013) reported model-based fluxes of 0.02–0.16 nmol N_2O m^{-2} s^{-1} at 10°E off Walvis Bay, and 0.2–0.3 nmol N_2O m^{-2} s^{-1} from shipboard observations on the shelf (13–14°E), which is consistent with our findings at 23°S (Figure 3). Contrarily, F_{N_2O} for the Cunene-Cape frio cells (maximum 1.33 nmol m^{-2} s^{-1}), and at 25°S (−0.03–0.33 nmol m^{-2} s^{-1}) were higher than those from Frame et al. (2014) for similar locations. The discrepancies can be associated with stronger upwelling during our cruises since, unlike previous studies, they took place during the seasonal peak of along-shore winds (Monteiro, 2010).

Our F_{N_2O} for the nBUS are comparable to those off Mauritania (Kock et al., 2012; Wittke et al., 2010), California (Lueker, 2004), and Mexico (Babbin et al., 2015), but lie within the lower range of estimates for the coastal upwelling off Peru (Arévalo-Martínez et al., 2015) and Chile (Cornejo et al., 2007; Paulmier et al., 2008; Table S1). Hence, our F_{N_2O} data suggest the nBUS to be, at the time of sampling, a rather moderate source of N_2O to the atmosphere. However, our cruises only covered part of the seasonal cycle and no events

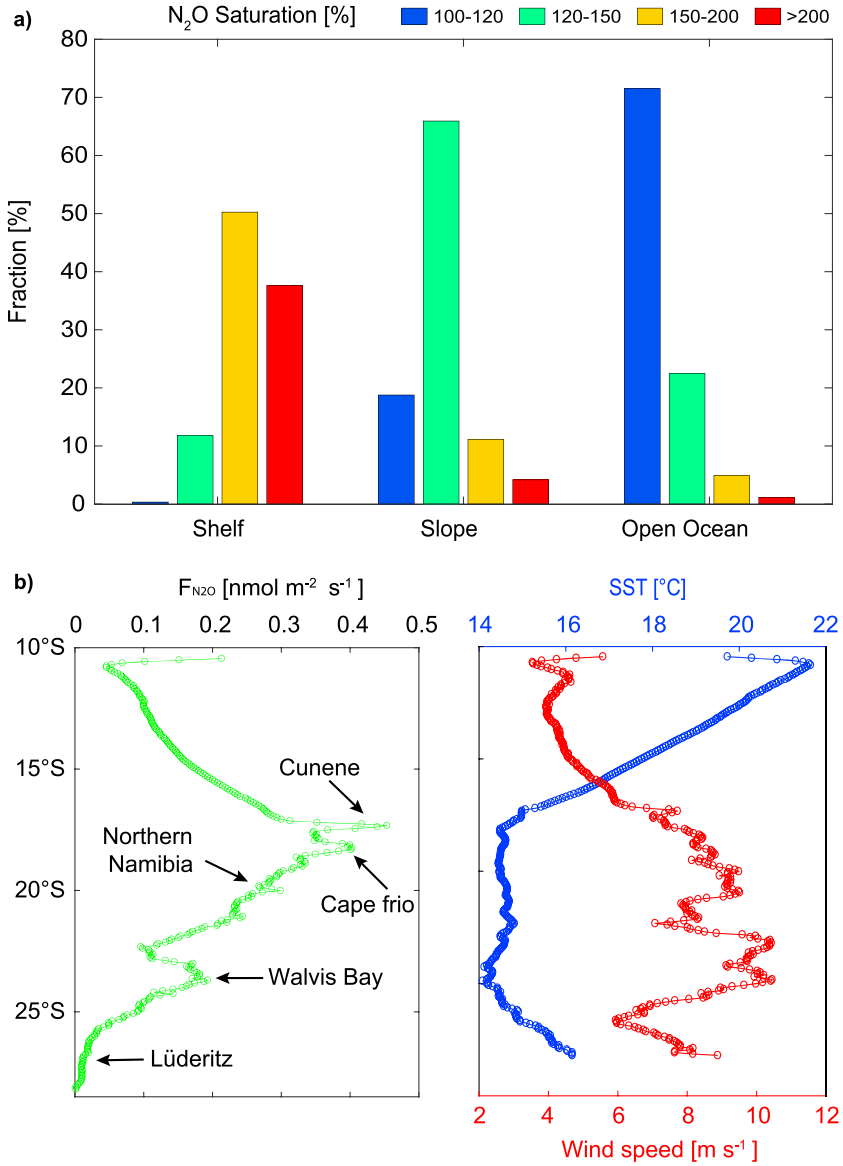

Figure 3. Spatial variability of N_2O during M98-M100/1. (a) Histogram showing the variable contribution of different areas to N_2O outgassing from the northern Benguela upwelling system. (b) Latitudinal distribution of F_{N_2O}, SST, and wind speeds across the Benguela upwelling system (zonal means at 1/32° spacing; 10.5–15°E). Main upwelling cells as in Figure 1. SST = sea surface temperature.

with drastic reductions in subsurface O_2 concentrations were observed. Since such events frequently occur during austral spring and summer (Mohrholz et al., 2008), it is likely that even higher N_2O concentrations could also be found seasonally in near-surface waters. On the other hand, as pointed out by Gutknecht, Dadou, Le Vu, et al. (2013), N_2O fluxes to the atmosphere in the nBUS do not necessarily reflect the magnitude of its subsurface production because a large fraction of these waters is advected from the coast. Future studies should set focus on assessing the magnitude of production and exchanges of N_2O in this region, and the fate of N_2O-rich waters advected by the AC.

3.3. Upwelling Filaments

Besides a clear seasonal cycle, biogeochemical processes in the nBUS are strongly influenced by short-term variability due to wind forcing and mesoscale dynamics (Mohrholz et al., 2014). Filaments are "finger-like" features which transport cold waters, tracers, and OM across the frontal zone in coastal upwelling systems (Hösen et al., 2016; Muller et al., 2013). Rees et al. (2011) showed that transient filaments off Mauritania may account for up to 1.2% of the global upwelling emissions of N_2O, suggesting that they should be included in

future assessments of its marine sources. Likewise, Lendt et al. (1999) reported a considerable enhancement in N_2O_{sat} for an upwelling filament off Oman, showing its relevance as a source of atmospheric N_2O.

In an attempt to quantify the effect of upwelling filaments in N_2O emissions from the nBUS, we computed a SST anomaly (SST_{anom}) with respect to mean ambient temperature using a similar approach as Hösen et al. (2016; supporting information S1). Using negative SST_{anom} <−0.25 °C and a meridional extent of 3–50 km as criteria, we identified 34 upwelling filaments. Although the extent of SST_{anom} was comparable throughout the nBUS at the time of sampling, in general the highest F_{N_2O} were associated with filaments north of 22°S (Figure S5). The wide range of values within this zonal band might result from the different ages of the filaments. For instance, Rees et al. (2011) observed a twofold to fourfold decrease in N_2O fluxes for a 2 weeks old filament. Although generally lower, F_{N_2O} south of 24°S were still positive and therefore their contribution should not be neglected (section 3.4).

Based on our data we cannot precisely quantify the F_{N_2O} change in surface waters advected within filaments considered in this study nor the effective area of enhanced fluxes. Likewise, the effect of progressive warming of the filaments (changing N_2O_{sat} without affecting the concentrations per se) was not accounted for. For instance, a twofold to threefold decrease in the maximal F_{N_2O} value of this study within 28 days (maximal filaments's lifetime in the nBUS; Hösen et al., 2016) would result in F_{N_2O} of 0.56–0.84 nmol m^{-2} s^{-1}, which are still higher than previous estimates. On the other hand, whereas the usual offshore limit of EBUS is set to 150 km (Chavez & Messié, 2009), most filaments in the nBUS reach 120–400 km offshore (Hösen et al., 2016). Thus, filaments are likely to expand the offshore extent of N_2O-outgasing waters.

3.4. Implications for Global Ocean N_2O Emissions

In order to compute regional emissions of N_2O, we binned our F_{N_2O} data in 1/32° boxes and estimated a per-area emission value for all boxes within 150 km from the coast (Figure S6). The resulting area (175,356 km^2; 16–28.5°S) is similar to that reported by Brown et al. (1991; 179,000 km^2), includes waters with maximal primary productivity (Chavez & Messié, 2009) and its seaward boundary represents the mean zonal extension of upwelling fronts in the BUS (Monteiro, 2010). Adding the values from all boxes resulted in emissions of 1.27×10^{-9} Tg-N_2O for our sampling period. Perennial coastal upwelling is the major process explaining the N_2O efflux in the nBUS and therefore it is reasonable to assume that, as an approximation, our estimate can be upscaled to a yearly basis. Doing so resulted in emissions of 0.040 Tg-N_2O per year with a range between 7.64×10^{-4} Tg-N_2O per year and 0.36 Tg-N_2O per year (boxes with the lowest and highest values, respectively). However, as mentioned above, upwelling filaments are likely to lengthen the high-N_2O emissions areas in offshore direction. After pooling in situ SST data in 1/32° boxes and flagging those with SST_{anom} <−0.25° (supporting information S1), we searched for areas which indicated the presence of upwelling filaments out of the 150 km limit (Figure S7). This resulted in an area of 21,717 km^2 whereby the emissions added to 0.0010 Tg-N_2O per year, increasing our original estimate by ca. 3%. It is noteworthy that the farthest filament signals were observed south of 24°S in connection with the Lüderitz cell. Hence, although emissions from the southern sector of the nBUS seem minor in comparison to the whole region, the persistency of the N_2O efflux to the atmosphere over longer distances and at higher temporal frequency at the Lüderitz cell might offset the effects of a lower air-sea gradient.

Our annual emission estimate (0.041 Tg-N_2O; 0.026 Tg-N) is 40% higher than what Nevison et al. (2004) reported for the coastal band between 5 and 30°S (0.025 ± 0.018 Tg-N_2O) despite their larger area. In comparison to the annual global ocean source of 4 Tg-N from the same study, our estimate suggests that the nBUS contributes 0.6% of that source, which is only a slight increase with respect to the reported 0.4%. Nevertheless, our results also indicate that the nBUS' share to the total source of N_2O from coastal upwelling (0.2 Tg-N; Nevison et al., 2004) lies around 13% and not 8% as previously suggested. Recently, Buitenhuis et al. (2018) suggested the contribution of coastal oceans to be much lower than assumed by Nevison et al. (2004; 2.5 Tg-N per year). However, a drawback of their estimates is the lack of near-coastal data as presented in this study. Furthermore, our estimate is conservative since our measurements do not cover the southern Benguela region (Lamont et al., 2015) where low-O_2 waters and upwelling potentially foster high N_2O production and fluxes to the atmosphere. Löscher et al. (2016) reported extreme N_2O concentrations at the fringes of bottom H_2S-containing waters on the Peruvian shelf. Given the widespread occurrence of sulphidic events in the BUS (Ohde & Dadou, 2018), it could be that such conditions enhance surface fluxes of N_2O as bottom waters are advected/mixed toward the surface. Nonetheless, we did not account for the seasonal-intraseasonal variability of upwelling, adding to the uncertainties of our annual efflux of N_2O.

Although N_2O emissions from the nBUS seem lower compared to other EBUS, its surface area is considerably smaller. Whether the contribution of the BUS could match other EBUS by considering its full extent and/or full seasonal cycles cannot yet be answered since, to date, there are not published measurements of N_2O in the southern Benguela region, and only a few cruises have measured in the nBUS. Hence, as for other EBUS (e.g., Arévalo-Martínez et al., 2015), N_2O emissions from the BUS might also need to be revised. Finally, it is also unclear how fast is the decay of F_{N_2O} within filaments and the spatial-temporal variability of the coastal sources of N_2O. Resolving these scales of variability is important given the episodic nature of upwelling events and the dominant role of intraseasonal variability in the BUS (Chavez & Messié, 2009). Analysis of small-scale N_2O changes during, for example, Lagrangian experiments might contribute to an improved estimation of N_2O emissions from the nBUS.

4. Conclusions

We present the first comprehensive survey of surface distribution and sea-to-air fluxes of N_2O in the nBUS. The regional variability of N_2O is driven by changes in upwelling and mixing at localized centers along the coast. In comparison to other EBUS, the nBUS is a moderate source of N_2O to the atmosphere (0.6–1.1% of the global ocean with reference to Nevison et al., 2004, and Buitenhuis et al., 2018, respectively). This contribution is not negligible since the nBUS represents <0.06% of the ocean's surface and it is therefore, disproportionally high. However, questions as to how is the balance between midwater advection versus surface mixing of N_2O produced in the OMZ, the extent of seasonal variability of F_{N_2O}, and the overall impact of upwelling filaments exporting N_2O-rich waters to the open ocean are still to be resolved. Despite the relevance of the BUS as a source of N_2O (and other greenhouse gases: Emeis et al., 2018; Monteiro et al., 2006; Santana-Casiano et al., 2009), this system is still highly undersampled. Given the widespread expansion of low-O_2 waters (Breitburg et al., 2018) and the predicted changes in intensity of upwelling-favorable winds in EBUS (Lamont et al., 2017; Sydeman et al., 2014; Wang et al., 2015), it seems timely to include N_2O in sustained monitoring programs to accurately assess the long-term trends of its emissions. Likewise, a better understanding of N_2O variability shall contribute to improve predictions on how the N-cycle will respond to ongoing global warming and ocean deoxygenation.

Acknowledgments
This study was funded by the joint projects SOPRAN III (FKZ 03F662A) and SACUS (03G0837A), the Future Ocean Excellence Cluster at Kiel University (CP0910) and the EU FP7 project InGOS (284274). We are grateful to the captains and crew of the RV Meteor for their assistance during the cruises. Likewise we thank the chief scientists of the M99 (D. Quadfasel) and M100/1 (F. Buchholz) cruises for their support. Special thanks to A. Flohr, T. Rixen, J. Werner, and M. Glockzin for providing technical support during M99-M100/1. Moreover, we thank G. Krahmann and J. Werner for providing processed thermosalinograph data. We also thank M. Dengler for his comments to an earlier version of the manuscript. The comments of two anonymous reviewers helped to improve the manuscript significantly. The underway N_2O data presented in this study will be archived in the MEMENTO (MarinE MethanE and NiTrous Oxide) database (https://memento.geomar.de) upon publication.

References

Arévalo-Martínez, D. L., Beyer, M., Krumbholz, M., Piller, I., Kock, A., Steinhoff, T., et al. (2013). A new method for continuous measurements of oceanic and atmospheric N_2O, CO and CO_2: Performance of off-axis integrated cavity output spectroscopy (OA-ICOS) coupled to non-dispersive infrared detection (NDIR). *Ocean Sciences*, *9*, 1071–1087.

Arévalo-Martínez, D. L., Kock, A., Löscher, C. R., Schmitz, R. A., & Bange, H. W. (2015). Massive nitrous oxide emissions from the tropical South Pacific Ocean. *Nature Geoscience*, *8*, 530–533. https://doi.org/10.1038/ngeo2469

Arévalo-Martínez, D. L., Kock, A., Steinhoff, T., Brandt, P., Dengler, M., Fischer, T., et al. (2017). Nitrous oxide during the onset of the Atlantic cold tongue. *Journal of Geophysical Research: Oceans*, *122*, 171–184. https://doi.org/10.1002/2016JC012238

Babbin, A. R., Bianchi, D., Jayakumar, A., & Ward, B. B. (2015). Rapid nitrous oxide cycling in the suboxic ocean. *Science*, *348*, 1127–1229.

Bange, H. W., Rapsomanikis, S., & Andreae, M. O. (1996). Nitrous oxide in coastal waters. *Global Biogeochemical Cycles*, *10*(1), 197–207. https://doi.org/10.1029/95GB03834

Behrenfeld, M. J., & Falkowski, P. G. (1997). Photosynthetic rates derived from satellite-based chlorophyll concentration. *Limnology and Oceanography*, *42*(1), 1–20.

Breitburg, D., Levin, L. A., Oschlies, A., Grégoire, M., Chavez, F. P., Conley, D. J., et al. (2018). Declining oxygen in the global ocean and coastal waters. *Science*, *359*, eaam7240. https://doi.org/10.1126/science.aam7240

Brown, P. C., Painting, S. J., & Cochrane, K. L. (1991). Estimates of phytoplankton and bacterial biomass and production in the northern and southern Benguela ecosystems. *South African Journal of Marine Science*, *11*(1), 537–564. https://doi.org/10.2989/025776191784287673

Buitenhuis, E. T., Suntharalingam, P., & Le Quéré, C. (2018). Constraints on global oceanic emissions of N_2O from observations and models. *Biogeosciences*, *15*, 2161–2175. https://doi.org/10.5194/bg-15-2161-2018

Capone, D. G., & Hutchins, D. A. (2013). Microbial biogeochemistry of coastal upwelling regimes in a changing ocean. *Nature Geoscience*, *6*, 711–717.

Carr, M.-E. (2002). Estimation of potential productivity in Eastern Boundary Currents using remote sensing. *Deep-Sea Research Part II*, *49*, 59–80.

Chavez, F. P., & Messié, M. A. (2009). Comparison of eastern boundary upwelling ecosystems. *Progress in Oceanography*, *83*, 80–96.

Chavez, F. P., & Toggweiler, K. (1995). Physical estimates of global new production: The upwelling contribution. In C. P. Summerhayes, K. -C. Emeis, M. V. Angel, R. L. Smith, & B. Zeitzschel (Eds.), *Upwelling in the ocean: Modern processes and ancient records* (pp. 313–320). Chichester: John Wiley.

Cornejo, M., Farías, L., & Gallegos, M. (2007). Seasonal cycle of N_2O vertical distribution and air-sea fluxes over the continental shelf waters off central Chile ($\sim 36°S$). *Progress in Oceanography*, *75*, 383–395.

Dlugokencky, E. J., Lang, P. M., & Masarie, K. A. (2014). Atmospheric N_2O dry air mole fractions from the NOAA GMD Carbon Cycle Cooperative Global Air Sampling Network. Version: May, Version: May 2014.

Elkins, J. W., Wofsy, S. C., McElroy, M. B., Kolb, C. E., & Kaplan, W. A. (1978). Aquatic sources and sinks for nitrous oxide. *Nature*, *275*, 602–606.

Emeis, K., Eggert, A., Flohr, A., Lahajnar, N., Nausch, G., Neumann, A., et al. (2018). Biogeochemical processes and turnover rates in the Northern Benguela Upwelling System. *Journal of Marine Systems*, *188*, 63–80. https://doi.org/10.1016/j.jmarsys.2017.10.001

Frame, C. H., Deal, E., Nevison, C. D., & Casciotti, K. L. (2014). N_2O production in the eastern South Atlantic: Analysis of N_2O stable isotopic and concentration data. *Global Biogeochemical Cycles*, *28*, 1262–1278. https://doi.org/10.1002/2013GB004790

Garrat, J. R. (1977). Review of drag coefficients over oceans and continents. *Monthly Weather Review*, *105*, 915–929.

Goreau, T. J., Kaplan, W. A., Wofsy, S. C., McElroy, M. B., Valois, F. W., & Watson, S. W. (1980). Production of NO_2^- and N_2O by nitrifying bacteria at reduced concentrations of oxygen. *Applied Environmental Microbiology*, *40*(3), 526–532.

Gruber, N., & Galloway, J. N. (2008). An Earth-system perspective of the global nitrogen cycle. *Nature*, *451*, 293–296.

Gutknecht, E., Dadou, I., Le Vu, B., Cambon, G., Sudre, J., Garçon, V., et al. (2013). Coupled physical/biogeochemical modeling including O_2-dependent processes in the Eastern Boundary Upwelling Systems: Application in the Benguela. *Biogeosciences*, *10*, 3559–3591.

Gutknecht, E., Dadou, I., Marchesiello, P., Cambon, G., Le Vu, B., Sudre, J., et al. (2013). Nitrogen transfers off Walvis Bay: A 3-D coupled physical/biogeochemical modeling approach in the Namibian upwelling system. *Biogeosciences*, *10*, 4117–4135.

Hansen, H. P. (1999). Determination of oxygen. In K. G. Grasshoff, K. Kremling, & M. Ehrhardt (Eds.), *Methods of seawater analysis* pp. 75–90). Weinheim, Germany: Wiley-VCH.

Hösen, E., Möller, J., Jochumsen, K., & Quadfasel, D. (2016). Scales and properties of cold filaments in the Benguela upwelling system off Lüderitz. *Journal of Geophysical Research: Oceans*, *121*, 1896–1913. https://doi.org/10.1002/2015JC011411

Hutchings, L., van der Lingen, C. D., Shannon, L. J., Crawford, R. J. M., Verheye, H. M. S., Bartholomae, C. H., et al. (2009). The Benguela current: An ecosystem of four components. *Progress in Oceanography*, *83*, 15–32.

Jury, M. R. (2017). Coastal upwelling at Cape Frio: Its structure and weakening. *Continental Shelf Research*, *132*, 19–28. https://doi.org/10.1016/j.csr.2016.11.009

Kämpf, J., & Chapman, P. (2016). *Upwelling systems of the world*, pp. 251–314. Switzerland: Springer International Publishing. https://doi.org/10.1007/978-3-319-42524-5

Kanamitsu, M., Ebisuzaki, W., Woollen, J., Yang, S.-K., Hnilo, J. J., Fiorino, M., & Potter, G. L. (2002). NCEP-DOE AMIP-II Reanalysis (R-2). *Bulletin of the American Meteorolical Society*, *83*, 1631–1643. https://doi.org/10.1175/BAMS-83-11-1631

Kock, A., Schafstall, J., Dengler, M., Brandt, P., & Bange, H. W. (2012). Sea-to-air and diapycnal nitrous oxide fluxes in the eastern tropical North Atlantic Ocean. *Biogeosciences*, *9*, 957–964.

Kopte, R., Brandt, P., Dengler, M., Tchipalanga, P. C. M., Macueria, M., & Ostrowski, M. (2017). The Angola Current: Flow and hydrographic characteristics as observed at 11°S. *Journal of Geophysical Research: Oceans*, *122*, 1177–1189. https://doi.org/10.1002/2016JC012374

Kuypers, M. M. M., Lavik, G., Woebken, D., Schmid, M., Fuchs, B. M., Amann, R., et al. (2005). Massive nitrogen loss from the Benguela upwelling system through anaerobic ammonium oxidation. *Proceedings of the National Academy of Sciences*, *102*(8), 6478–6843.

Lamont, T., García-Reyes, M., Bograd, S. J., van der Lingen, C. D., & Sydeman, W. J. (2017). Upwelling indices for comparative ecosystem studies: Variability in the Benguela Upwelling System. *Journal of Marine Systems*, *188*, 3–16. https://doi.org/10.1016/j.jmarsys.2017.05.007

Lamont, T., Hutchings, L., van den Berg, M. A., Goschen, W. S., & Barlow, R. G. (2015). Hydrographic variability in the St. Helena Bay region of the southern Benguela ecosystem. *Journal of Geophysical Research: Oceans*, *120*, 2920–2944. https://doi.org/10.1002/2014JC010619

Lendt, R., Hupe, A., Ittekkot, V., Bange, H. W., Andreae, M. O., Thomas, H., et al. (1999). Greenhouse gases in cold water filaments in the Arabian Sea during the southwest monsoon. *Naturwissenschaften*, *86*, 489–491.

Löscher, C. R., Bange, H. W., Schmitz, R. A., Callbeck, C. M., Engel, A., Hauss, E., et al. (2016). Water column biogeochemistry of oxygen minimum zones in the eastern tropical North Atlantic and eastern tropical South Pacific oceans. *Biogeosciences*, *13*, 3585–3606.

Lueker, T. J. (2004). Coastal upwelling fluxes of O_2, N_2O and CO_2 assessed from continuous atmospheric observations at Trinidad, California. *Biogeosciences*, *1*, 101–111. https://doi.org/10.5194/bg-1-101-2004

Lutjeharms, J. R. E., & Meeuvis, J. M. (1987). The extent and variability of South-East Atlantic upwelling. *South African Journal of Marine Science*, *5*(1), 51–62. https://doi.org/10.2989/025776187784522621

Mohrholz, V., Bartholomae, C. H., van der Plas, A. K., & Lassa, H. U. (2008). The seasonal variability of the northern Benguela undercurrent and its relation to the oxygen budget on the shelf. *Continental Shelf Research*, *28*, 424–441.

Mohrholz, V., Eggert, A., Junker, T., Nausch, G., Ohde, T., & Schmidt, M. (2014). Cross shelf hydrographic and hydrochemical conditions and their short term variability at the northern Benguela during a normal upwelling season. *Journal of Marine Systems*, *140*, 92–110.

Mohrholz, V., Schmidt, M., & Lutjeharms, J. R. E. (2001). The hydrography and dynamics of the Angola-Benguela Frontal Zone and environment in April 1999. *South African Journal of Marine Science*, *97*(5), 199–208.

Monteiro, P. M. S. (2010). The Benguela Current System. In K.-K. Liu, L. Atkinson, R. A. Quiñones, & L. Taleue-McManus (Eds.), *Carbon and nutrient fluxes in continental margins: A global synthesis* (pp. 65–78). Springer.

Monteiro, P. M. S., & van der Plas, A. K. (2006). Low oxygen water (LOW) variability in the Benguela System: Key processes and forcing scales relevant to forecasting. In V. Shannon, G. Hempel, P. Malanotte-Rizzoli, C. Moloney, & J. Woods (Eds.), *Large Marine Ecosystems* (Vol. 14, pp. 71–90). Amsterdam: Elsevier.

Monteiro, P. M. S., van der Plas, A. K., Mohrholz, V., Mabille, E., Pascall, A., & Joubert, W. (2006). Variability of natural hypoxia and methane in a coastal upwelling system: Oceanic physics or shelf biology *Geophysical Research Letters*, *33*, L16614. https://doi.org/10.1029/2006GL026234

Morgan, E. J., Lavric, J. V., Seifert, T., Chicoine, T., Day, A., Gomez, J., et al. (2015). Continuous measurements of greenhouse gases and atmospheric oxygen at the Namib Desert Atmospheric Observatory. *Atmospheric Measurement Techniques*, *8*, 2233–2250.

Muller, A. A., Mohrholz, V., & Schmidt, M. (2013). The circulation dynamics associated with a northern Benguela upwelling filament during October 2010. *Continental Shelf Research*, *63*, 59–68. https://doi.org/10.1016/j.csr.2013.04.037

Myhre, G. D., Schindell, D., Bréon, F.-M., Collins, W., Fuglestvedt, J., Huang, J., et al. (2013). Anthropogenic and natural radiative forcing. In T. F. Stocker, D. Qin, G.-K. Plattner, M. Tignor, S. K. Allen, J. Boschung, et al. (Eds.), *Climate change 2013: The physical science basis, contribution of working group I to the fifth assessment report of the intergovernmental panel on climate change* (pp. 129–234). United Kingdom and New York (USA): Cambridge University Press, Cambridge.

Nagel, B., Emeis, K.-C., Flohr, A., Rixen, T., Schlarbaum, T., Mohrholz, V., & van der Plas, A. (2013). N-cycling and balancing of the N-deficit generated in the oxygen minimum zone over the Namibian shelf–An isotope based approach. *Journal of Geophysical Research: Biogeosciences*, *118*, 361–371. https://doi.org/10.1002/jgrg.20040

Nevison, C. D., Lueker, T. J., & Weiss, R. F. (2004). Quantifying the nitrous oxide source from coastal upwelling. *Global Biogeochemical Cycles*, *18*, GB1018. https://doi.org/10.1029/2003GB002110

Ohde, T., & Dadou, I. (2018). Seasonal and annual variability of coastal sulphur plumes in the northern Benguela upwelling system. *PLoS ONE*, *13*(2), e0192140. https://doi.org/10.1371/journal.pone.0192140

Paulmier, A., Ruiz-Pino, D., & Garçon, V. (2008). The oxygen minimum zone (OMZ) off Chile as an intense source of CO_2 and N_2O. *Continental Shelf Research*, *28*, 2746–2756.

Pierrot, D., Neill, C., Sullivan, K., Castle, R., Wanninkhof, R., Lüger, H., et al. (2009). Recommendations for autonomous underway pCO_2 measuring systems and data-reduction routines. *Deep-Sea Research Part II*, *56*, 512–522.

Ravishankara, A. R., Daniel, J. S., & Portmann, R. W. (2009). Nitrous oxide (N_2O): The dominant ozone-depleting substance emitted in the 21st Century. *Science*, *326*, 123–125.

Rees, A. P., Brown, I. J., Clark, D. R., & Torres, R. (2011). The Lagrangian progression of nitrous oxide within filaments formed in the Mauritanian upwelling. *Geophysical Research Letters*, *38*, L21606. https://doi.org/10.1029/2011GL049322

Santana-Casiano, J. M., González-Dávila, M., & Ucha, I. R. (2009). Carbon dioxide fluxes in the Benguela upwelling system during winter and spring: A comparison between 2005 and 2006. *Deep-Sea Research Part II*, *56*, 533–541. https://doi.org/10.1016/j.dsr2.2008.12.010

Schafstall, J., Dengler, M., Brandt, P., & Bange, H. W. (2010). Tidal-induced mixing and diapycnal nutrient fluxes in the Mauritanian upwelling region. *Journal of Geophysical Research*, *115*, C10014. https://doi.org/10.1029/2009JC005940

Seitzinger, S. P., Kroeze, C., & Styles, R. V. (2000). Global distribution of N_2O emissions from aquatic systems: Natural emissions and anthropogenic effects. *Chemosphere*, *2*, 267–279.

Shannon, L. V., Agenbag, J. J., & Buys, M. E. L. (1987). Large- and mesoscale features of the Angola-Benguela Front. South African *Journal of Marine Science*, *5*(1), 11–34. https://doi.org/10.2989/025776187784522261

Suntharalingam, P., Buitenhuis, E., Le Quéré, C., Dentener, F., Nevison, C. D., Butler, J. H., et al. (2012). Quantifying the impact of anthropogenic nitrogen deposition on oceanic nitrous oxide. *Geophysical Research Letters*, *39*, L07605. https://doi.org/10.1029/2011GL050778

Sydeman, W. J., García-Reyes, M., Schoeman, D. S., Rykaczewski, R. R., Thompson, S. A., Black, B. A., & Bograd, S. J. (2014). Climate change and wind intensification in coastal upwelling ecosystems. *Science*, *345*, 77–80.

Tchipalanga, P., Dengler, M., Brandt, P., Kopte, R., Macuéria, M., Coelho, P., et al. (2018). Eastern boundary circulation and hydrography off Angola—Building Angolan oceanographic capacities. *Bulletin of the American Meteorological Society*, *99*, 1589–1605. https://doi.org/10.1175/BAMS-D-17-0197.1

Trenberth, K. E., Large, W. G., & Olson, J. G. (1990). The mean annual cycle in global ocean wind stress. *Journal of Physical Oceanography*, *20*, 1742–1760. https://doi.org/10.1175/15200485(1990)020b1742:TMACIGN2.0.C02

Voss, M., Bange, H. W., Dippner, J. W., Middelburg, J. J., Montoya, J. P., & Ward, B. (2013). The marine nitrogen cycle: Recent discoveries, uncertainties and the potential relevance of climate change. *Philosophical Transactions of the Royal Society of London B*, *368*(1621). https://doi.org/10.1098/rstb.2013.0121

Wang, D., Gouhier, T. C., Menge, B. C., & Ganguly, A. R. (2015). Intensification and spatial homogenization of coastal upwelling under climate change. *Nature*, *518*, 390–394.

Wittke, F., Kock, A., & Bange, H. W. (2010). Nitrous oxide emissions from the upwelling area off Mauritania. *Geophysical Research Letters*, *37*, L12601. https://doi.org/10.1029/2010GL042442